Time-Bound Optimal Planning in CNC Machine Considering Machining Safety

Jianxin Guo, Mingyong Zhao, and Lixian Zhang

***Abstract*— In this paper, we propose a time-bound optimal planning model to reconcile the dilemma between the cutting efficiency and the cutting security. Unlike the traditional planning method, we consider the bound of the kinematic constraints to be flexible in the form of a fuzzy set. It is reasonable to use such an expression considering that the safety of the computer numerical control (CNC) machine is susceptible to the potential disturbance in the cutting process. A fuzzy optimization method is used to obtain a compromise bound aiming to balance the cutting efficiency and the cutting security. The original problem can be reduced into a convex problem in some weak conditions, for which some interesting results are proved and the numerical method is also used to solve it. The proposed algorithm is experimented on our self-designed CNC machine. We verify the effectiveness of our proposed method through air-cutting and milling process with two respect experiment, and verify the efficiency of our algorithm by comparing traditional open-loop strategies.**

***Note to Practitioners*—The starting point of this article is to improve the safety performance under the premise of ensuring the efficiency of CNC machining, but this method is also applicable to other robot arm path planning and design. The boundary of the existing speed planning problem cannot guarantee the safety of the machining process, and blindly reducing the kinematic boundary will greatly sacrifice the processing efficiency. This paper proposes a new method based on fuzzy programming to determine the optimal kinematic boundary, and this process can be completely realized in an open-loop manner, avoiding the method of avoiding risks through machine reorganization. In this paper, we mathematically describe the conditions for forming flexible kinematic boundaries, and then we resolve this problem into a fast-solvable optimization problem through a series of transformations. We perform air-cutting on the formed machining paths, incorporate them into the CAD system or carry out pocket milling tests in production. Preliminary physical experiments show that this method is feasible and has unique advantages over existing open-loop methods. In future research, we will give a more accurate estimate of the security membership function and extend the method to higher-order kinematically constrained problems.**

Manuscript received 29 August 2023; accepted 12 October 2023. This article was recommended for publication by Associate Editor N. Frigerio and Editor J. Li upon evaluation of the reviewers' comments. This work was supported by the National Natural Science Foundation of China under Grant 72171222. *(Corresponding author: Jianxin Guo.)*

Jianxin Guo is with the Institutes of Science and Development, Chinese Academy of Sciences, Beijing 100190, China (e-mail: guojianxin@casisd.cn).

Mingyong Zhao is with BKLPUMEC, Department of Mechanical Engineering, Tsinghua University, Beijing 100084, China.

Lixian Zhang is with the Academy of Mathematic and Systems Science, Chinese Academy of Sciences, Beijing 100190, China.

Color versions of one or more figures in this article are available at https://doi.org/10.1109/TASE.2023.3324849.

Digital Object Identifier 10.1109/TASE.2023.3324849

***Index Terms*— Velocity planning, flexible kinematic bound, open-loop strategy, milling operation.**

I. Introduction

AS AN advanced manufacturing technology, CNC machine tools are widely used in the fields of machinery manufacturing, automobile industry, aerospace and intelligent robot automatic production, and play an important role in intelligent manufacturing. For example, in the field of machinery manufacturing, as the demand for mechanical precision parts becomes more and more diverse and personalized. The precision machining of these parts can be realized by applying the numerical control machining technology on the numerical control machining equipment, which meets the needs of fast product update and high precision. For another example, in the field of aerospace, the demand for high-precision and differentiated parts is increasing rapidly, involving large parts such as wings and fuselages, and processing of complex curved surfaces such as propellers and turbine blades. These parts have high requirements for strength, stiffness and reliability. It is very high, but the material has poor rigidity and complex structure, which cannot be completed on ordinary machine tools. High-end CNC machine tools can meet the processing requirements of high speed, high precision and high flexibility.

Therefore, the comprehensive performance of CNC machining equipment, including the size of the machining area, cutting torque, rigidity, etc., has also become more and more strict [1]. If high-value parts have processing safety problems, or even be damaged due to equipment failure, it will not only cause huge direct economic losses and production interruptions, but also slow down the development of manufacturers. However, the fact is that the current machine tool design rarely considers the impact of various failures on product quality. Even if the failure probability of the machine tool itself is small, the supply of external causes such as grid instability may still cause equipment failure. In addition, machine design is also difficult to change after installation. In particular, some old machine tool manufacturers may have gone bankrupt, so parts manufacturers cannot get technical support. At this time, there is a very urgent need to add preventive measures for processing risks. Therefore, a more effective type of solution in practice is to start reducing the machining quality risk of the part during the machining design stage and take related preventive measures.

Based on the above facts, this study proposes an operation-friendly strategy that can be implemented in the

open-loop phase of velocity planning to control machining risks. Considering that excessive processing speed is the main cause of wear, tool breakage and shutdown accidents during processing, here we intend to control the existing processing risks from the aspect of speed planning. The price of improving processing safety is sacrificing part of the processing speed, or processing efficiency. However, we try to give a reasonable trade-off strategy for this decision to ensure the maximum possible efficiency improvement within a certain security range.

To achieve this, we employ a time-optimal velocity planning framework. Since the speed bound determines the maximum speed of the processing process, a reasonable boundary decision means the corresponding processing safety level. In fact, the kinematic boundary of velocity planning was proposed early to suppress vibration to a certain extent [2]. Moreover, in some cases, the preference index during processing can be understood as a linear combination of certain kinematics and dynamics [3]. Based on this idea, it is theoretically feasible to understand the safety of the machining process as a mapping of certain kinematics of the planning process. Specifically, we realize the combination of kinematic bounds and temporal optimization through the technique of fuzzy optimization [4], so that a reasonable set of Pareto bounds is selected for the cutting process. We have carried out some theoretical analysis of the model, and found that this framework can be finally classified into a class of traditional speed optimal control problems. In the end, we achieved the desired result through several stages including: de-fuzzy the original model to be "crisp", normalizing the objective function, and non-linear optimization algorithms. Overall, our approach here is easier to implement for work related to traditional CNC failover. We know that mechanical adjustment is the most direct way to solve related problems. But this method requires dismantling the mechanical structure, which is very expensive to maintain. In addition, the method here is also an extension of the speed planning algorithm, which is more flexible than technologies such as filters.

II. Literature Review

The literature involved in this work comes from two general directions, one strand is related to speed planning. Traditionally, time-optimal feedrate planning along a given parametric tool path is of significant importance for achieving this goal in the CNC systems ([5], [6], [7], [8]). The feedrate planning problem is usually formulated as a time-minimum optimal control problem under kinematic constraints such as confined feedrate, axis acceleration, jerk, and even jounce, and efficient algorithms have been proposed to solve the problem. The acceleration bounds are introduced to reduce inertia and prevent mechanical shocks. The jerk and jounce bounds are used to generate smooth feedrate profiles aimed at improving the machining quality. Different models and algorithms have been designed to obtain feedrate planning. For instance, [9] discussed a sequential algorithm for the computation of a minimum-time speed profile over a given path. Reference [10] proposed an integrated jerk-limited method of minimal time trajectory planning with confined contour error. Reference [11] proposed a novel feedrate scheduling method for generating smooth feedrate profile conveniently with the consideration of both chord error and kinematic error. In fact, the velocity curve obtained by this basic planning algorithm is still easily affected by external shock and structural vibration. Some work on modifying the input curves to suit the machining characteristics also accompanies them. Well-known techniques such as input shaping ([12]), or Finite Impulse Response (FIR) filtering ([13], [14]) have been integrated to minimize residual vibrations. However, filtering introduces unavoidable delay and induces large contouring errors in multi-axis motion that must be compensated ([15]). Alternatively, it is reasonable to integrate the handing method into the planning process which is before the cutting process. Such strand involves the error compensation consideration. For instance, [16] proposed a double Taylor expansion-based contouring error estimation method for spatial contours; [17] presents a new contour error pre-compensation method that integrates analytical prediction of contour error, optimal path-reshaping model for five-axis machining; [3] incorporate the axis error constraints into the conventional feedrate planning model to cope with the inaccuracy problem in the cutting process.

The other strand is risk assessment and management for CNC. According to the view in [18], in actual CNC engineering problems, most of the occurrence of a fault has an interaction, and hence the traditional methods cannot identify the interaction between faults. Thus, correct corrective measures cannot be taken, resulting in repeated faults in the use of products, thus reducing the reliability of product. For this reason, many decision evaluation models in fault diagnosis have been developed accordingly. Reference [19] proposed Interpretive Structural Modeling (ISM)/Analytical Network Process (ANP) Accurately to describe the relationship between CNC equipment failures and identify reliability weakness. In the study of [20], the explanatory structural model approach was adopted to realize the hierarchical structure of the fault propagation model through matrix transformation and decomposition. In order to accurately describe and explore the relationship between CNC equipment faults and identify the weak links of reliability, a new method for CNC equipment related fault analysis based on social network analysis (SNA) was proposed in [21]. Reference [22] proposed a comprehensive risk assessment model in which multiple techniques are combined to generate a Failure Mode and Effects Analysis (FMEA) model for generating a comprehensive failure mode ranking. Risk management is also a difficult task relative to risk identification. It is often necessary to estimate the likelihood of occurrence and impact on the manufacturing process during the risk assessment phase to prioritize risks and to determine the most appropriate risk mitigation strategy during the mitigation phase [23]. There are many strategies to ensure the safety of CNC machining. For instance, A 3D vision-based time-of-flight sensor is proposed in [24] to provide in-depth information about the manufacturing scene, which can be used by the proposed method to make effective decisions to automatically detect and avoid collisions for safe toolpaths in the production process. Reference [25] presented an optimization method for CNC high-quality operation to

obtain optimal machining process parameters. Reference [26] proposed a method to satisfy a given spindle power constraint during the optimization process by iteratively adjusting the value of the feedrate plan in each production cycle. In addition, there has also recently been work on safety assurance for robots similar to CNC. For instance, a safe Bayesian optimization algorithm has been developed, which guarantees that the performance of the system never falls below a critical value [27]. Generally speaking, there is relatively more work on risk identification, while the work on safety management focuses on virtual scenes (CAD/CAM process) and tool parameter optimization.

III. Time-Bound Optimal Planning Model With Fuzzy Kinematic Constraints

In this section, we propose a practical model to reconcile the efficiency-security dilemma. Aim to describe the flexible bound set for the constraints, we will introduce the fuzzy set theory which helps to model the problem. To begin with, we introduce some basic concept about the fuzzy set.

A. Fuzzy Set Theory Principles

Let X be the universal set with its elements denoted by x. Membership of the element x to a classical subset G (also known as crisp set G) of X is defined by the following characteristic function:

$$\mu_G(x) = \begin{cases} 1, & x \in G, \\ 0, & x \notin G. \end{cases}$$

When the valuation set $\{0, 1\}$ is replaced by the closed set $[0, 1]$, we can define a fuzzy set A through its membership function $\mu_A(x)$. It associates with each element x in X a real number in the interval $[0, 1]$. Therefore, A is completely characterized by the following description set:

$$A = \{[x, \mu_A(x)] : x \in X, 0 \le \mu_A(x) \le 1\}.$$

For instance, if we choose $X = \mathscr{R}$, $A = \mathscr{R}^+ \cup \{0\}$, and the membership of A to be (in Fig.1):

$$\mu_A(x) = \begin{cases} 1, & 0 \le x \le 1, \\ \frac{1}{2} - \frac{1}{2}\sin(x - \frac{3}{2})\pi, & 1 < x \le 2, \\ 0, & x > 2. \end{cases}$$

Thus, $\mu_A(\frac{3}{2}) = \frac{1}{2}$, $\mu_A(\frac{7}{4}) = \frac{1}{2} - \frac{\sqrt{2}}{4}$, $\mu_A(3) = 0$. We can find in this case, $3 \notin A$, and $\frac{3}{2}, \frac{7}{4} \in A$ however $\frac{3}{2}$ belongs to A "more than" $\frac{7}{4}$ belongs to A. In a word, the concept of the fuzzy set is an extension to the classical set, i.e. it not only defines which element belongs to the set but also describe how much it belongs to this set. Always, in the following discussion we denote the fuzzy set A to be $\tilde{A}$.

B. Crisp Kinematic Constraints

In CNC domain time-optimal planning problem is of significant importance, which has attracted many researchers. The goal of that is to generate the feedrate to finish the given cutting curve under the given kinematic information and other constraints. The bound of the constraints is predefined considering the mechanical properties of the machine tool and the lathe itself. Mathematically, it can be described as following:

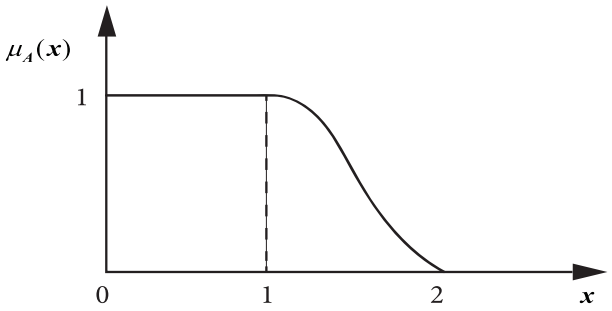

Fig. 1. Membership function defined upon $\mathscr{R}^+ \cup \{0\}$.

$$\min T \ s.t. \ |v_\tau| \le V_{\max}, |a_\tau| \le A_{\max} \qquad \text{(III.1)}$$

The numerical solution of this problem can be perfectly solved through many methods like [5] and [6]. For concision, we denote this problem to be $\boldsymbol{P_0}$.

We assume that the value of the bound $V_{\max}$ and $A_{\max}$ are to be chosen from $\mathscr{V}$ and $\mathscr{A}$. It is easy to find that given the bound values $(V_{\max}, A_{\max}) \in \mathscr{V} \times \mathscr{A}$, a feasible solution v, a, T can be expressed as the function of the bound pair $(V_{\max}, A_{\max})$. This means that there exists an "induced projection" $\mathscr{F}$ from the pair of bound setting value $\mathscr{V} \times \mathscr{A}$ to the solution space (v, a, or T):

$$\mathscr{F}_s : \mathscr{V} \times \mathscr{A} \to \mathscr{S}.$$

This means that $\mathscr{F}_s(V_{\max}, A_{\max}) = s, s = v, a, T$. Here, without loss the generality we denote $s = v, a, T$ in the solution space $\mathscr{S}$. Thus, we can view this problem from another angle, i.e. $v = v(V_{\max}, A_{\max}), a = a(V_{\max}, A_{\max})$, and $T = T(V_{\max}, A_{\max})$. Correspondingly, an optimal solution (local or global) from that can also be denoted as: $v^* = v^*(V_{\max}, A_{\max}), a^* = a^*(V_{\max}, A_{\max}), T^* = T^*(V_{\max}, A_{\max})$.

C. Fuzzy Kinematic Constraints

In the practice, the bound of the velocity and the acceleration are predefined through considering the ability of the lathe and the machine tool from the history evidence or experience. It is inapplicable to adopt a fixed bound to implement the velocity planning considering the potential risk during the cutting process. The fixed bound can easily bring about the negative consequence such as the vibration, severe wear or poor accuracy. All of these negative it may generate is named as the "insecurity consequence" in this paper. Here, we intend to ensure a conservative bound though it may sacrifice an allowable cutting time in order to reconcile the efficiency and the security dilemma.

Via the fuzzy set theory, we consider the bound pair $(V_{\max}, A_{\max}) \in \mathscr{V} \times \mathscr{A}$ to be defined upon a fuzzy set, and also we denote a corresponding membership function $\mu_s, s = v, a, T$ as well. Specifically, the membership function is endowed with a special meaning, i.e. it denotes the security level about each kinematic variable $s \in \mathscr{S}$. If $\mu_s = 0$,

it denotes under this condition the choice of s is "riskiest"; when $\mu_s = 1$, it denotes under this condition the choice of s is "safest". Besides, the rest "fuzzy situation" parallels to the number $\mu_s \in (0, 1)$.

Based on the angle above, we describe the imprecise right-hand side by fuzzy sets. Thus the fuzzy model of the time optimal problem can be drawn as:

$$\min T \ \ s.t. \ |v_\tau| \tilde{\leq} \tilde{V}_{max}, |a_\tau| \tilde{\leq} \tilde{A}_{max}. \tag{III.2}$$

The "$\tilde{\leq}$" is a comparison symbol in the meaning of fuzzy set, which is defined according to the membership function of velocity and acceleration, i.e. $\mu_v(x)$ and $\mu_a(x)$. For further preparation, we have to predefine the sliding window of $V_{\max}$ and $A_{\max}$, which requires that the permissable relaxed value must be given. Thus if we assume that $\mathscr{V} = [V_{\max}, V_{\max} + dV]$ and $\mathscr{A} = [A_{\max}, A_{\max} + dA]$, the membership function of $s = v, a$ can be obtained:

$$\mu_v(x) = \begin{cases} 1, & x < V_{\max}, \\ \mu_1(x), & V_{\max} \leq x \leq V_{\max} + dV, \\ 0, & V_{\max} + dV < x. \end{cases}$$

$$\mu_a(x) = \begin{cases} 1, & x < A_{\max}, \\ \mu_1(x), & A_{\max} \leq x \leq A_{\max} + dA, \\ 0, & A_{\max} + dA < x. \end{cases}$$

Here $\mu_i, i = 1, 2$ are two decreasing continuous function; $V = V_{max}, A = A_{max}$ are the safest limitations; dV, dA are the permissive slipping bounds. In order to further obtain relevant theoretical results, we need to make the following assumptions.

Assumption 1: $\mu_i, i = 1, 2$ are non-increasing functions.

This is mainly based on the experience that the higher the speed, the faster the tool wear and the shorter the service life. Compared with the machining form, the influence of cutting speed and tool material on the tool wear mechanism is more prominent ([28], [29]). For example, among physical models describing tool life, an important branch is around Taylor's tool life equation ([30]), which relates tool life to cutting speed in a reverse exponential relationship. Latest development on Taylor's equation can be found in [31]. Hence, here we can assume that the relationship between the maximum speed of the tool and the safety membership function is non-increasing.

D. Problem Conversion

It is not always to solve the fuzzy optimization problem (III.2), however in most case which can be converted into a MO (multi-objective) optimization by considering the following relationship:

$$x \tilde{\leq} \tilde{V} \Leftrightarrow \begin{cases} x \leq V + dV, \\ Max\{\mu_v(x)\}. \end{cases}$$

$$x \tilde{\leq} \tilde{A} \Leftrightarrow \begin{cases} x \leq A + dA, \\ Max\{\mu_a(x)\}. \end{cases}$$

Here dV and dA are given. We found that while relaxing the boundary of kinematics, we introduced a corresponding indicator function, which are μ_v and μ_a.

This conversion can be understood in this way, we need to choose a certain boundary that meets the needs from a more relaxed boundary. This required boundary is characterized by the value of the membership function. This method de-fuzzy the right side of the inequality however introducing additional optimization goal. Properly speaking, one fuzzy inequality claims one optimization goal. Accompanied by the defuzzification of kinematic constraints, it is also necessary to defuzzify the objective function. Although the original objective function is deterministic, after the kinematics fuzzy side is determined, the objective function needs to be considered within the more relaxed constraints, i.e., the corresponding membership function μ_J is required. For convenience, we define $J = -T$, then the fuzzy optimization problem (III.2) can be converted into the following MO problem:

$$\begin{aligned} &Max\{\mu_J\}, Max\{\mu_v(v_\tau)\}, Max\{\mu_a(a_\tau)\} \\ &s.t \ |v_\tau| \leq V_{\max} + dV, |a_\tau| \leq A_{\max} + dA. \end{aligned} \tag{III.3}$$

Remark 3.1: We have to clarify the fact that if $x(u)$ is a function with respect to parameter $u \in \Gamma$, then $\mu_v(x)$ is a set, which is defined as $\mu_v(x) = \{\mu_v(x(u)) | u \in \Gamma\}$. Correspondingly, at this time, $\max\{\mu_v(x)\} = \max\{\mu_v(x(u)) | u \in \Gamma\}$. The same definition is also valid for μ_a.

We will discuss how to define μ_J. At this point, the choice of the membership function of the objective function is more subjective, which we will discuss in detail later in the experimental part. Here we discuss theoretically how to choose the membership function of the objective function. Intuitively speaking, it is similar to the membership function of the kinematics constraint, we need to first calculate the value range of the index function. According to the characteristics of the time-optimal problem, we can easily find that these two boundaries should be the solutions of the following two problems $\boldsymbol{P_1}$ and $\boldsymbol{P_2}$:

$$\boldsymbol{P_1}: \begin{array}{l} Max \ J \\ s.t \\ |v_\tau| \leq V, |a_\tau| \leq A. \end{array} \qquad \boldsymbol{P_2}: \begin{array}{l} Max \ J \\ s.t \\ |v_\tau| \leq V + dV, |a_\tau| \leq A + dA. \end{array}$$

Hence, considering each bound pair $(V_{\max}, A_{\max}) \in \mathscr{V} \times \mathscr{A}$ to be defined upon a fuzzy set corresponding to a certain index J, we can define the membership function of the objective function as following:

$$\mu_J(x) = \begin{cases} 0, & x < J^-, \\ \mu_0(x), & J^- \leq x \leq J^+, \\ 1, & J^+ < x. \end{cases}$$

Here, J^- and J^- are the corresponding solution of $\boldsymbol{P_1}$ and $\boldsymbol{P_2}$; $\mu_0(x)$ is an increasing function to be given. Therefore, the original fuzzy problem is transformed into a Problem(III.3).

Problem (III.3) is a standard multi-objective optimization, which is the computational process of simultaneously optimizing two or more conflicting objectives subject to a set of constraint functions. Gerenally, for non-trivial multi-objective problems, there is not a single solution that simultaneously optimizes all objectives. Instead, there is set of solutions for which, when attempting to improve an objective, other objectives get worse. These solutions are called Pareto optimal or Pareto efficient solutions. The solution methods can

be categorized into many groups including methods with a priori articulation of preferences, methods for a posteriori articulation of preference, methods with no articulation of preferences and genetic algorithms. Most of these either reflect decision-maker's priori or posteriori preferences to represent the complete Pareto optimal set. Given the variety of methods in this section, the question arises as to which method is the best. Unfortunately, there is no distinct answer. In this paper, from the practical angle as well as the induction facility we adopt Max-Min method, which is a method with no articulation of preferences. It is worth mentioning that the analysis in the following part is representative, similar results can also be established through other multi-objective optimization conversion method. Hence, we consider the following max-min problem (MMP):

$$\begin{aligned} &Max\ Min\ \{\mu_J, \mu_v(v_\tau), \mu_a(a_\tau)\} \\ &s.t\ \ |v_\tau| \le V + dV, |a_\tau| \le A + dA. \end{aligned} \tag{III.4}$$

Thus if we define:

$$\lambda = Min\ \{\mu_J, \mu_v(v_\tau), \mu_a(a_\tau)\},$$

then the Max-Min problem (III.4) can be reduced into a crisp single objective optimization:

$$Max\ \lambda \quad s.t \begin{cases} |v_\tau| \le V + dV, \\ |a_\tau| \le A + dA, \\ \lambda \le \mu_0(J), \\ \lambda \le \mu_1(|v_\tau|), \\ \lambda \le \mu_2(|a_\tau|), \\ 0 \le \lambda \le 1. \end{cases} \tag{III.5}$$

we denote which as $\lambda - MMP$ or $\boldsymbol{Q_0}$. The conversion is based on the Lemma below, detail about which can be referred to [32].

Lemma 3.2: The optimal problem MMP (III.4) is equal to $\lambda - MMP$ (III.5).

E. Property of the Converted Problem

In this section, our aim is to establish the relationship between the proposed model and the traditional one. As what we have discussed above, the Max-Min conversion is one of the considered methods, however whose exploring techniques is representative. Thus, we take interest in some properties of the $\lambda - MMP$. To begin with, we introduce some useful concepts and lemmas:

Lemma 3.3: The optimal velocity curve of the problem $\boldsymbol{P_0}$ is unique and maximum at each point.

Proof: According to the result from [8]. ■

Definition 3.4: For any pair V_{max}, A_{max}, problem $\mathbf{P_0}(V_{max}, A_{max})$ is bang-bang with respect to velocity and acceleration, if and only if the velocity(axis or both) and acceleration(axis or both) curve of the optimal solution from this problem reach their bounds both. We call this situation the "same bang-bang", or "S-bang-bang".

We have to make a detailed description of this definition. The "bang-bang" defined here is unlike the traditional definition, which is much more strong. As it is know to all, in the acceleration constraint case, the traditional bang-bang will surely occur, i.e. acceleration must reach its bound alternatively. However, S-bang-bang also claims that the velocity reaches its bound even if there is just one point on the velocity curve reaches the bound. We have to give an assumption as a fundamental hypothesis to develop a key theorem.

Assumption 2: If the problem $\mathbf{P_0}(V + dV, A)$ is S-bang-bang, thus for any pair $(V_{max}, A_{max}) \in \mathscr{V} \times \mathscr{A} = [V, V + dV] \times [A, A + dA]$, $\mathbf{P_0}(V_{max}, A_{max})$ is also S-bang-bang. Especially at this time, we say $\mathscr{V} \times \mathscr{A}$ is cross-valid.

This assumption can ensure the S-bang-bang occurring in a domain if the pair of the upper bound of $\mathscr{V}$ and the lower bound of $\mathscr{A}$ is S-bang-bang. Intuitively, this inference established itself in one dimension, nevertheless this assumption is a little strong in some sense. The case becomes much more complex in the multi-axis case, and strict proof is to be given. However, the assumption used here will not undermine the universal property of the following results.

Lemma 3.5: Supposing that $\mathscr{V} \times \mathscr{A} = [V, V + dV] \times [A, A + dA]$ is cross-valid, thus for $\mathbf{P_0}(V_{max}, A_{max})$, denote functions with two variables:

$$\pi_s = Min\mu_s(\mathscr{F}_s(V_{max}, A_{max})).$$

Here, $s = v, a, j$. Thus π_v and π_a are continuous functions with respect to V_{max} and A_{max} respectively; π_j is strict monotonous function with respect to (V_{max}, A_{max}).

Proof: It is easy to check that $\pi_v = Min\mu_v(v(V_{max}, A_{max})) = \mu_v(Max v(V_{max}, A_{max})) = \mu_v(V_{max})$. The first equation holds because of the definition of $\mathscr{F}_s$, the second equation holds because that μ_v is a decreasing function, and the last equation holds because that $\mathscr{V} \times \mathscr{A} = [V, V + dV] \times [A, A + dA]$ is cross-valid. It is continuous under the definition of μ_v. The affirmation establishes to π_a as well.

Besides, according to Lemma (3.3) it is easy to verify that π_j is strict monotonous function with respect to (V_{max}, A_{max}). ■

Assumption 3: π_j is continuous with respect to (V_{max}, A_{max}).

In fact, Assumption 2 is necessary for us to develop the following ratiocination, which is weak however can not always holds since we know the monotonous property does not implies the continuity. Based upon the condition above, we can obtain the following interesting properties.

Theorem 3.6: Under Assumption 1 and Assumption 2, if s^* is the optimal solution of the $\lambda - MMP$, then π_{s^*} are the same.

Proof: According to the denotation, we only have to prove that

$$\pi_j^* = \mu_j(J(V_{max}^*, A_{max}^*)), \pi_v^* = \mu_v(V_{max}^*), \pi_a^* = \mu_a(A_{max}^*)$$

are the same.

In the light of Lemma (3.5) and the Assumption 1 and Assumption 2, we can conclude that π_v is decreasing if and only if V_{max} is increasing, π_a is decreasing if and only if A_{max} is increasing, and π_j is strictly decreasing if and only if either

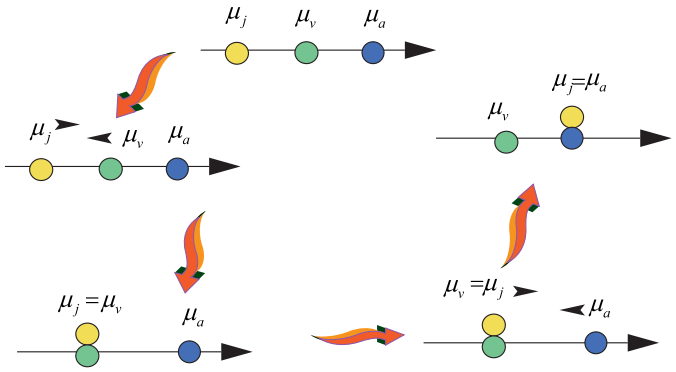

Fig. 2. Illustration of the proof in Theorem (3.6). Given any three different initial values of μ_s, the optimal value can always be found by fixing one of them and transforming the other two values. In fact, it is always possible to obtain the same value for all three μ_s at the optimum point after a finite number of steps.

V_{max} or A_{max} is increasing. Thus, we can obtain that if π_v or π_a is increasing (or decreasing), then π_j is decreasing (or increasing).

Considering the meaning of $\lambda-MMP$, according to Lemma (3.5) it is equal to find an optimal solution that maximize the minimal among π_s. We consider such a case, in the optimal point if π_j is the smallest one, say $\pi_j < \pi_v$. Thus, let us fix A_{max}, and then as V_{max} increasing π_v will decreasing and π_j will increasing. In the light of Assumption 2, there exists such a time that $\pi_j = \pi_v$. In this time, this renewed state (π_s) is obviously much more optimal than the initial one. This is a contradiction to the definition of the optimal solution of $\lambda - MMP$. Likewise, if $\pi_j > \pi_v$ we can adopt the same strategy to fine another feasible solution of $\lambda-MMP$ which is supreme than the original one. This means the optimal solution of $\lambda - MMP$ must have the property that $\pi_j = \pi_v$.

Similarly, π_a can not be the minimal or maximal strictly too. Based on the analysis above, the proof is complete. ■

Remark 3.7: Theorem (3.6) is a very important result, which demonstrate a necessary condition for the optimal solution with respect to the proposed model. Besides, it is very convenient for us to check this feature from the optimal solution. In the result section, we will test this necessary condition to verify the effectiveness of the model as well as the numerical method.

IV. Functional Forms and Parametrization

A. Set Function Selection

Decision in a fuzzy environment is given as an option that simultaneously fulfills the goal and the constraints of the problem. Therefore the optimal decision to our problem should be the element that has the highest membership degree in the fuzzy set intersection of fuzzy sets representing the objective function and the constraints ([33], [34], [35]). According to our theory the set function for velocity and acceleration must reflect the "safety" concern, which are claimed to be decreasing about these kinematic bounds as the penalty. However, the set function for the optimal index must be the otherwise situation. Generally speaking, the choice for this function is not univocal as long as it can be applied to indicate the interpretation between the safety and the kinematic bound. To verify the effectiveness in our model, the set function we choose here for $\mu_0(x), \mu_1(x), \mu_2(x)$ are monotonous and linear, which maybe the simplest forms to meet the requirement of the properties:

$$\begin{cases} \mu_0(x) = \dfrac{x}{dJ} - \dfrac{J}{dJ}, x \in [J, J+dJ], \\ \mu_1(x) = \dfrac{(V+dV)^2}{(V+dV)^2 - V^2} - \dfrac{x}{(V+dV)^2 - V^2}, \\ x \in [V^2, (V+dV)^2], \\ \mu_2(x) = \dfrac{A+dA}{dA} - \dfrac{x}{dA}, x \in [A, A+dA]. \end{cases} \tag{IV.1}$$

Noticing here that the constraint $|v_\tau| \le V + dV$ has been replaced with $|v_\tau|^2 \le (V+dV)^2$, because the latter form is more convenient for us to implement the numerical in the following procedure. With this transformation, constraints on velocity can be expressed linearly.

B. Problem Reformulation

Under our choice of the function form, the corresponding constraints in Problem (III.5) can be equivalent to:

$$\mu_0(-T) \ge \lambda \Leftrightarrow \frac{(-T)}{dJ} - \frac{J}{dJ} \ge \lambda \Leftrightarrow \lambda dJ + J + T \le 0.$$

Considering $v_\tau = v_\tau(u)$,$a_\tau = a_\tau(u)$, then for every $u \in [0,1]$ we have:

$$\begin{aligned} \mu_1(|v_\tau^2|) \ge \lambda &\Leftrightarrow \frac{(V+dV)^2}{(V+dV)^2 - V^2} - \frac{|v_\tau^2|}{(V+dV)^2 - V^2} \ge \lambda \\ &\Leftrightarrow \lambda(2V+dV)dV + |v_\tau^2| \le (V+dV)^2, \\ \mu_2(|a_\tau|) \ge \lambda &\Leftrightarrow \frac{A+dA}{dA} - \frac{|a_\tau|}{dA} \ge \lambda \Leftrightarrow \lambda dA \\ &\quad + |a_\tau| \le A + dA. \end{aligned}$$

Thus, the final form of the original problem can be described in the following form:

$$Max \lambda \quad s.t \begin{cases} |v_\tau^2| \le (V+dV)^2, \\ |a_\tau| \le A + dA, \\ \lambda dJ + J + T \le 0, \\ \lambda(2V+dV)dV + |v_\tau^2| \le (V+dV)^2, \\ \lambda dA + |a_\tau| \le A + dA, \\ 0 \le \lambda \le 1. \end{cases} \tag{IV.2}$$

in which $v_\tau = v_\tau(u)$,$a_\tau = a_\tau(u)$; and here the function inequality hold for each $u \in [0,1]$.

C. Parameterization

In this section, we will rewrite problem in a discrete form which is more convenient for numerical solution. Denoting "$'$" to be "$\frac{\mathrm{d}}{\mathrm{d}u}$", we introduce another two new functions $a(u), b(u)$ with respect to parameter u:

$$a(u) = \dot{u}(u)^2 = \left(\frac{du}{dt}\right)^2,$$

$$b(u) = \ddot{u} = \frac{\mathrm{d}\dot{u}}{\mathrm{d}t} = \frac{1}{2}\left(\dot{u}^2\right)' = \frac{1}{2}a'(u).$$

Thus, the kinematic quantities can be written as functions with respect to a, b:

$$v_\tau = \tau' \dot{u} = \tau' \sqrt{a(u)},$$
$$a_\tau = \tau'' \dot{u}^2 + \dot{\tau} \dot{u} = \tau'' a(u) + \tau' b(u).$$

where $\tau \in \{x, y\}$.

Based upon the preparation above, the infinite optimization Problem (IV.2) can be approximately converted to a finite state optimization problem. Preliminarily, the parametric interval $[0, 1]$ is divided into N equal parts with knots $u_i = \frac{i}{N}$, $i = 0, 1, \ldots, N$. The length of each sub-interval is $\Delta = \frac{1}{N}$. Thus, if Δ is sufficient small, the constraints can be approximately transformed into a discrete inequalities at each point u_i. Therefore, we use $b_i = b(u_i), i = 0, \ldots, N$ as the control variables and the state variables $a_i = a(u_i), i = 0, \ldots, N$ can be calculated via $b_i \approx \frac{a_{i+1} - a_i}{2\Delta}$. Noting that the initial values of $a(u)$ are $a(0) = a(1) = 0$, for $i = 1, \ldots, N-1$, we have $a_{i+1} = 2\Delta \sum_{k=1}^{i} b_k$. As a consequence, Problem (IV.2) can be approximated by the following finite programming problem:

$$Max \lambda$$
$$s.t \quad \begin{cases} |\tau_i'^2 a_i(u)| \le (V + dV)^2 \\ |\tau_i'' a_i(u) + \tau_i' b_i(u)| \le A + dA \\ \lambda dJ + J \le (-\sum \frac{1}{\sqrt{a_i(u)}}) \\ \lambda(2V + dV)dV + |\tau_i'^2 a_i(u)| \le (V + dV)^2 \\ \lambda dA + |\tau_i'' a_i(u) + \tau_i' b_i(u)| \le A + dA \\ 0 \le \lambda \le 1 \end{cases} \tag{IV.3}$$

in which $\tau \in \{x, y\}$, $i = 0, \ldots, N$.

D. Property of the Solution

Similar to the discussion in the traditional optimal time planning with kinematic constraint problem, in this section we intend to establish the existence and the uniqueness condition of the Problem (IV.3). To begin with, we confirm that if the solution of the Problem (IV.3) exists, then it is global.

Lemma 4.1: The problem $\lambda - MMP$ (IV.3) is a convex optimization.

Proof: The optimized variables are $b_i(u)$ and λ. Since the variables $a_i(u)$ are the linear combination of $b_i(u)$, thus it only has to verify the left side of the following constraint is convex:

$$\lambda dJ + J + \sum \frac{1}{\sqrt{a_i(u)}} \le 0.$$

This is equal to that $\sum_{j=1}^{i} \frac{1}{\sqrt{a_j(u)}}$ is convex about $b_i(u)$ and λ. Further, if we prove that for any given i, $f = \frac{1}{\sqrt{a_i(u)}}$ is convex and then we can obtain the conclusion considering the linear combination of the convex function is still a convex function. In fact, we can calculate that: $\frac{\partial^2 f}{\partial b_j \partial b_k} = \frac{3}{4} a_i^{-\frac{5}{2}} \left(\frac{\partial a_i}{\partial b_j} \frac{\partial a_i}{\partial b_k} \right)$, $\frac{\partial^2 f}{\partial b_j \partial \lambda} = 0$ and $\frac{\partial^2 f}{\partial \lambda^2} = 0$. Accordingly, the Hessian Matrix $\mathscr{H}$ of the function f is:

$$\mathscr{H} = \frac{3}{4} a_i^{-\frac{5}{2}} \begin{pmatrix} \frac{\partial^2 a_i}{\partial b_1^2} & \cdots & \frac{\partial a_i}{\partial b_1} \frac{\partial a_i}{\partial b_N} & 0 \\ \cdots & \cdots & \cdots & 0 \\ \frac{\partial a_i}{\partial b_N} \frac{\partial a_i}{\partial b_1} & \cdots & \frac{\partial^2 a_i}{\partial b_N^2} & \cdots \\ 0 & 0 & \cdots & 0 \end{pmatrix}_{(N+1)\times(N+1)}$$

Hence, $\mathscr{H} = \frac{3}{4} a_i^{-\frac{5}{2}} \eta^T \eta$ is a positive semi-definite matrix, where $\eta = \left(\frac{\partial a_i}{\partial b_1} \ \frac{\partial a_i}{\partial b_2} \ \cdots \ \frac{\partial a_i}{\partial b_N} \ 0 \right)$. As mentioned above, this completes our proof. ■

Thus, we can draw the following result without render any proof.

Lemma 4.2: The optimal solution of the $\lambda - MMP$ (IV.3) is global.

In fact, the discrete form we used here can be applied the traditional problem $\mathbf{P_0}$ obviously. Here, what intrigues us most is the relationship between these two solution, which will be manifested in the following Lemma.

Lemma 4.3: The optimal solution of the $\lambda - MMP$ (III.5) is one optimal solution from $\mathbf{P_0}$ (in its discrete form).

Proof: Let $\lambda = Min\{\pi_j^*, \pi_v^*, \pi_a^*\}$ is the optimal solution of $\lambda - MMP$ (III.5). At this time, we choose the upper bound of solution with its velocity and acceleration as $\mu_v^{-1}(\pi_v^*)$ and $\mu_a^{-1}(\pi_a^*)$. The denotation $\mu_s^{-1}(\cdot)$ here means the reverse function of $\mu_s(\cdot)$, which is reasonable because of the monotonicity of the set function. Thus, we only have to prove that $\mu_j^{-1}(\pi_j^*)$ is the optimal index with respect to the Problem $\mathbf{P_0}(\mu_{\mathbf{v}}^{-1}(\pi_{\mathbf{v}}^*), \mu_{\mathbf{a}}^{-1}(\pi_{\mathbf{a}}^*))$.

On the contrary, if not, consider the optimal solution index $J^* = J(\mu_v^{-1}(\pi_v^*), \mu_a^{-1}(\pi_a^*))$ with respect to the problem $\mathbf{P_0}(\mu_{\mathbf{v}}^{-1}(\pi_{\mathbf{v}}^*), \mu_{\mathbf{a}}^{-1}(\pi_{\mathbf{a}}^*))$. Recalling that $J^* = -T^*$, hence due to its optimality, we have

$$J(\mu_v^{-1}(\pi_v^*), \mu_a^{-1}(\pi_a^*)) > \mu_j^{-1}(\pi_j^*).$$

This means we find a three-number set $(\mu_j(J^*), \pi_v^*, \pi_a^*)$, which is a feasible solution of $\lambda - MMP$ (III.5),i.e. there exists $\bar{\lambda} = Min\{\mu_j(J^*), \pi_v^*, \pi_a^*\}$. Thus, according to the proof process in Theorem (3.6), λ can not be the optimal solution for the $\lambda - MMP$ (III.5). Combined with the Lemma (4.2), we can obtain the contradiction. ■

So far, we have obtained several lemmas and results, which are contributed to the final result. The following result entails the existence and the uniqueness of the proposed model, which is also the foundation to ensure the further numerical method.

Theorem 4.4: The optimal solution of the $\lambda - MMP$ exists, and moreover it is unique.

Proof: The existence can be obtained from the proof process in Lemma (4.3) or (3.6). Besides, according to Lemma (4.3) we can see the solution of $\lambda - MMP$ is just a solution in $\mathbf{P_0}$, which is unique according to Lemma (3.3). ■

V. Algorithm Implementation

The entire problem-solving route is shown in the Fig.(3), and we will explain it step by step.

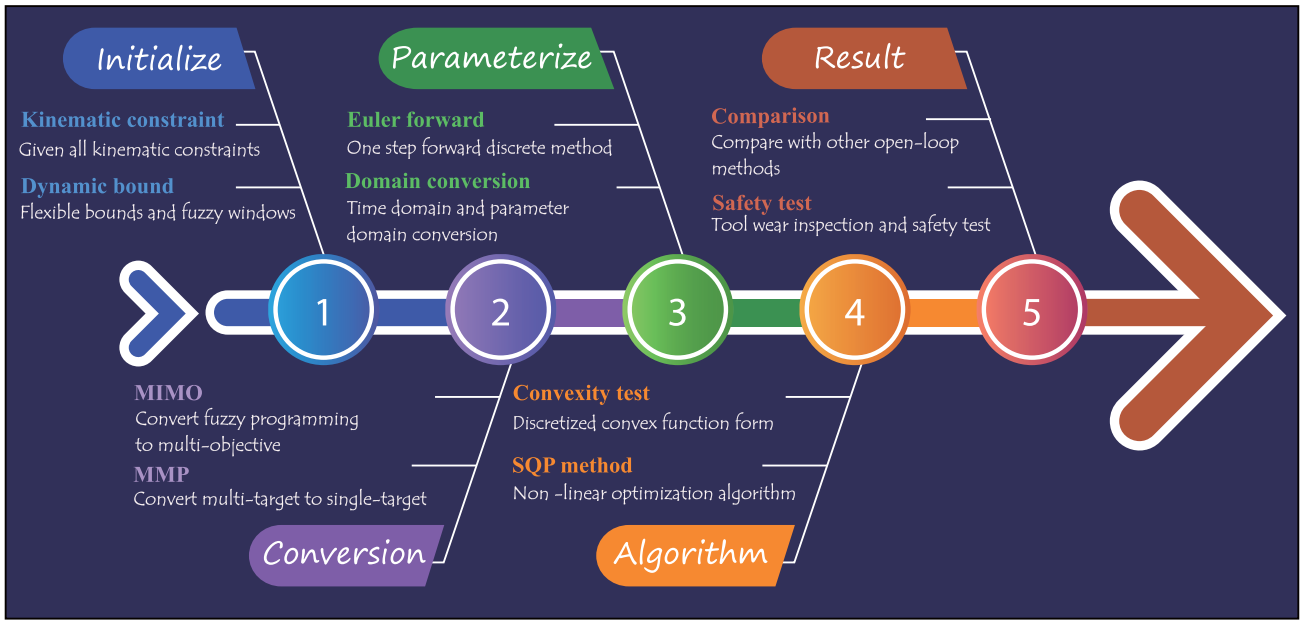

Fig. 3. Model and algorithm flowchart.

A. Algorithm Description

According to the final Problem (IV.3), a convex programming can be written as following.

$$Min\ c^T\mathbf{x}$$
$$s.t.\quad \begin{cases} A\mathbf{x} \le b; \\ f(\mathbf{x}) \le 0; \\ L \le \mathbf{x} \le U. \end{cases}$$

Here c, b, L and U are constant column vectors; A is constant matrixes; f is a convex function and x is the decision variable vector. Moreover, $\mathbf{x} = [b_1(u), b_2(u), \ldots, b_n(u), \lambda]^T$, and all of the const vectors and matrixes can be calculated according to the constraint conditions in model (IV.3). Besides, we can find the only nonlinear inequility in the programming is $\lambda dJ + J \le (-\sum \frac{1}{\sqrt{a_i(u)}})$, which is contained in the function $f(\mathbf{x})$. Compared with the tradition work such as [3], we can confirm that there is no significant difference in the computational complexity. The efficiency of the algorithm will be discussed further in the next subsection. In the light of the result in Theorem (4.4), we can turn to the numerical method solve the Problem (IV.3), which in fact is based on the algorithm in section III-C and the sequential quadratic programming (SQP) ([36]). All the numerical solution processes are running in Matlab environment, personal PC with 32-bit system, 2.10 GHz inter(R) Core(TM)2 Duo T6570 processor, and 2GB of RAM memory. After the optimal solution obtained by solving the convex programming problem (IV.3), the axis velocity at each sampling positions can be obtained by calculating $\dot{u}_i = \sqrt{a_i(u)}$. Using cubic B-spline to fit the velocity parameter curve, we can obtain the final velocity profile with the given interpolation time.

B. Algorithm Efficiency

As we have described in the previous section, the proposed model can reconcile the dilemma involving the kinematic performance and security performance. According to the result in Theorem (3.6) and the Definition (3.4), the result of the planning curves are also "bang-bang" or "S-bang-bang". The algorithm indeed helps us to find a reasonable bound in the sense of the safety. In order to use the SQP method to solve Problem (IV.3), the number N of discretizations need to be given. The selection of N is closely related to the lengths $\Delta s_i = r(u_i) - r(u_{i-1})$ of the line segments $r(u_i)r(u_{i+1})$. According to the theory of the finite element method, these lengths need to satisfy $\Delta s_i \le 0.1\ mm$ in order to achieve high-accuracy computation for most CNC machining. Hence, a lower bound N_l for N is the smallest integer such that $\Delta s_i \le 0.1\ mm$ for $i = 1, \ldots, N$. Furthermore, N should be large enough for the tool-path to be sufficiently subdivided. Combining these two factors, an experimental lower bound for $N = Max\{50, N_l\}$.

In this section, we select the number of the discretied points to compromise between accuracy and efficiency. When considering both accuracy and efficiency, the lower bound N_l are chosen from 100 to 800, with which we can test the planning time using the algorithm. As we have known, a low discrete level can result in an unsmooth curve, especially for the acceleration at the bang-bang switching junction. This natural dent on the curve can break the intended bound in the planning process, though in a small magnitude. We introduce the overshoot off the bound to be a criterion to test the planning accuracy. The related result are illustrated in the Table (I). The time is recorded after the implementation of the programming by 50 steps.

We can find that the numerical efficiency will be decreasing drastically as the N_l increasing. This is mainly due to the nonlinear part in the programming. However, it can be viewed from the results that the optimal index will be stable after the 200 discretizations, and at the same time the corresponding planning time and the overshoot are satisfied.

TABLE I
ALGORITHM EFFICIENCY TO SOLVE THE PROBLEM (IV.3)

N_l	Planning time(s)	Acceleration overshoot(%)	Optimal index(λ^*)
50	5.10	8.5	0.66
100	13.99	6	0.65
200	42.03	3.5	0.64
400	165.18	2	0.63
800	717.87	1	0.63

C. Experiment Setup

In this section, we use the proposed method to cope with a practical problem. The cutting curve "Hat" is in Fig.(6) generated using a spinle with the knots and the coefficients as follows:

Knots:

$$[0, 0, 0, 2/48, 10/48, 14/48, 20/48, \\ 28/48, 30/48, 32/48, 40/48, 1, 1, 1].$$

Coefficients:

$$\begin{bmatrix} 0 & -60 & -20 & 0 & 60 & 60 & 20 & 20 & 0 \\ 0 & 20 & 20 & 60 & 60 & 0 & -20 & -60 & 0 \end{bmatrix}.$$

We consider the kinematic constraints in three situations:

(1) the safest case: $V_{max} = 100mm/m$, $A_{max} = 300mm/m^2$;

(2) the riskiest case: $V_{max} = 150mm/m$, $A_{max} = 600mm/m^2$.

(3) the fuzzy case: the slip window are $dV = 50mm/m$, $dA = 300mm/m^2$.

The choice of membership function usually requires more considerations. As discussed in Section (III-C), empirical methods and statistical procedures are important methods for constructing membership functions. If we have further tool and material information, we can construct other types of fuzzy functions to better reflect the characteristics of the problem, for instance [37] and [38]. No matter what kind it chooses, the form must comfort to Assumption (1). However, without further information on the machine and tool material, it is sufficient to use linear features to represent its safe motion boundaries. In this way, we only need to calculate the values of the two endpoints of the membership function. By solving the two optimization problems in Eq.(IV.1), we can obtain the corresponding kinematic membership function and index membership function according to the formula Eq.(IV.1) as in Fig.(4).

The initial and terminal axis velocities and axis accelerations are all zero. The number N of discretizations is set to be 200 in the algorithm. A man-made CNC machine is used here to implement the experiment, whose implementation principle is illustrated in Fig.(5). The interpolation time chosen here is set as 0.01s, and the encoder is set to capture the output location. To illustrate the velocity and acceleration clearly, a filter algorithm is also used to depict the final result.

VI. RESULTS AND DISCUSSION

In this section, we conduct two sets of experiments on the described problems. The first set of experiments is to use the CNC in Fig.(5) for air cutting. Here, we intend to describe the cutting path, but do not cut the specific object. In the second set of experiments, we perform pocket milling with the milling tool manufactured by cemented caribide method, and analyzed it by observing the smoothness of the cutting objects under different kinematic constraints. Finally, we compare and discuss other open-loop methods.

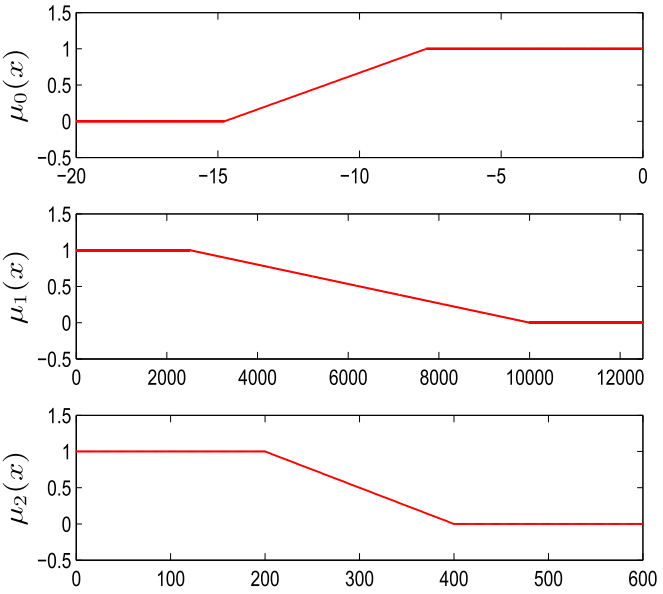

Fig. 4. Set functions.

A. Air-Cutting Result

Fig.(7) and Fig.(8) are the velocities and accelerations with the safest and riskiest bound under air cutting. Viewed from the pictures, we can see the solutions are bang-bang, i.e. at any time, either velocity or acceleration reach their bound, in fact which correspond to the traditional case described in Lemma (3.3). Also, we can find that the solutions are "S-bang-bang" in the light of our theory (3.4). Thus, it is also reasonable for us to choose these two bounds, which lays the foundation of Assumption (2) and hence the solution domain $\mathscr{V} \times \mathscr{A}$ is cross-valid. Besides, the cutting time are 3.46s and 5.56s respectively. We can see that it will sacrifice the cutting time to a great extent though using the safest bound can ensure that the CNC machine functions well.

Fig.(9) are the velocities and accelerations with flexible bounds. Through the fuzzy optimization method we obtain the recoiling bound of the kinematic constraints as $V = 72mm/s$, $A = 269mm/s^2$. We can find that the structure of the solutions are the same as the traditional ones. In fact, according to our results above (Lemma (4.3)), the results must be bang-bang. Besides, it is easy to check that the cutting time is 4.52s and the corresponding safety index about the optimal index is $J = -T$, in which the velocity safety index and the acceleration safety index are the same, namely:

$$\lambda^* = Min\{\pi_j^*, \pi_v^*, \pi_a^*\} = \pi_j^* = \pi_v^* = \pi_a^* = 0.64.$$

This result verifies our important result Theorem (3.6).

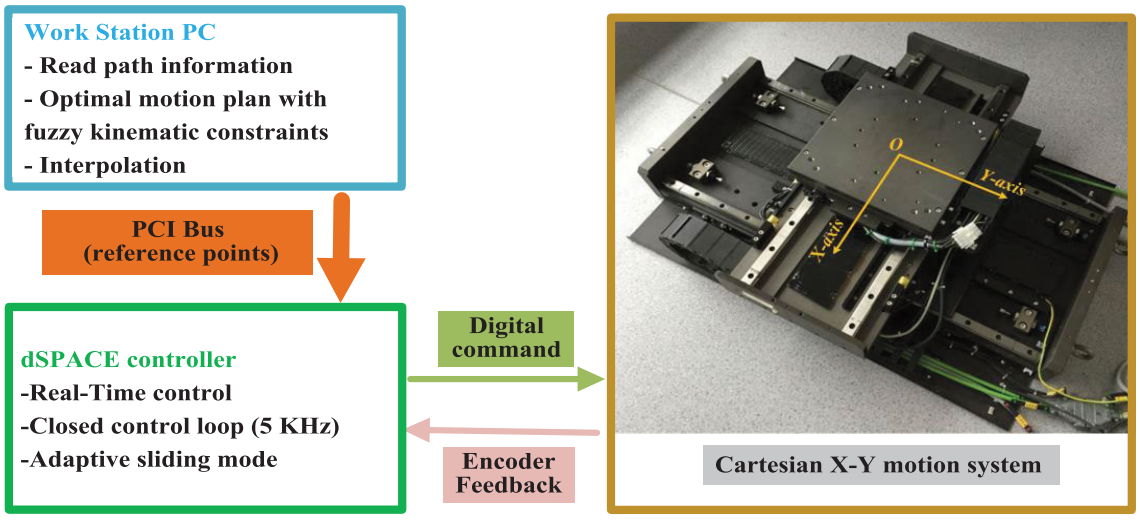

Fig. 5. CNC machine used in the experiment.

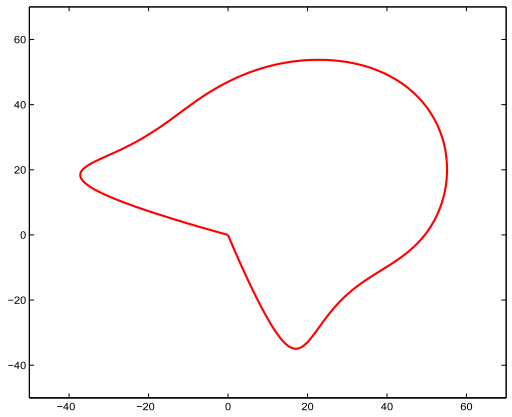

Fig. 6. Hat curve.

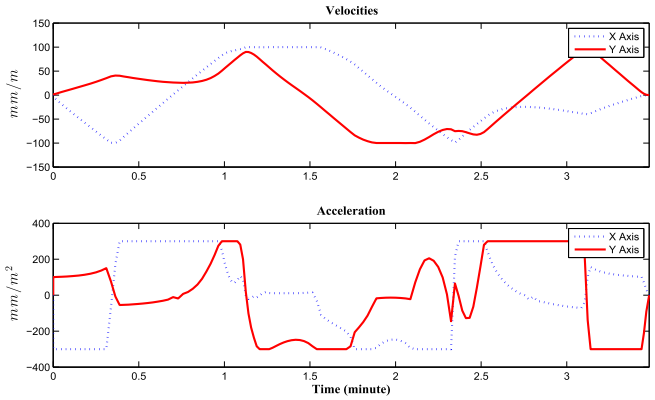

Fig. 7. Safest bound solution.

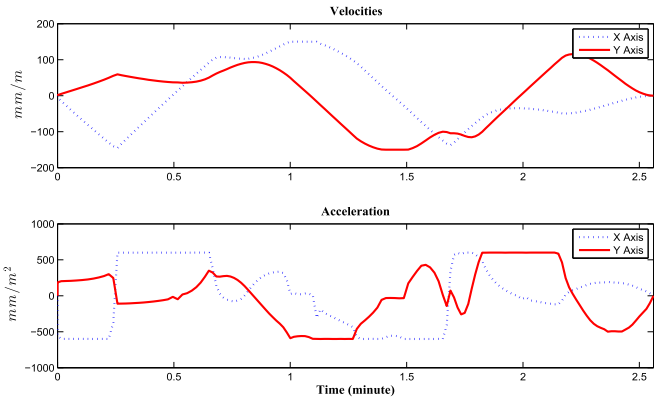

Fig. 8. Riskiest bound solution.

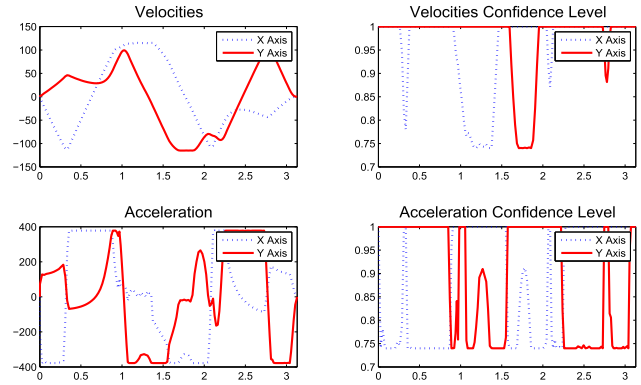

Fig. 9. Fuzzy bound solution.

B. Milling Process and Safety Test

To assess safety of machine tools and all the consumables (e.g. tools) a simple target machining operation (e.g. milling) should be considered. We use pocket milling operations which require speed and acceleration profiles to be properly handled, to avoid vibrations and quick tool wear phenomenon like cutting edge notching. In this section, we perform pocket milling with the proposed algorithm, and the milling tool is manufactured by cemented carbide. The milling results are illustrated in Fig.(10): from left to right—risk bound, safe bound, fuzzy bound— the red circled area we illustrate in picture show the smoothness of machined parts.

Here we reflect the safety level of the processing process by measuring the surface roughness. On the surface of a machined part, there will always be many small uneven peaks and valleys. The degree of these uneven peaks and valleys is the so-called surface roughness of the part. The surface roughness

Fig. 10. Milling results from left to right: risk bound, safe bound, fuzzy bound.

of machining is caused by plastic deformation during cutting separation, high-frequency vibration of the process system, friction between the tool and the machined surface, etc. For precision parts, the surface roughness should be reduced as much as possible to improve the surface quality of the parts. This is also an important criterion for measuring the quality of machining. For example, due to the vibration generated by the high speed, streaks or corrugated marks will be drawn on the processed surface, and the surface roughness value will increase significantly.

We found that when the bound with the highest risk, that is, the largest kinematic bound, there are obviously a lot of rough fine lines in the circled area of the machined part, indicating that there are various rough patterns. In the same area, when using the safest kinematic bound, these rough markings become blurred or disappear (middle image). When we use fuzzy kinematic bound, the level of object wear is in between. Some wear features are still present in the lower circled area, but the article is overall smoother in the upper circled area.

C. Comparison

In this section, we compare our method with the other representative open-loop optimization method proposed in [3] and [39]. We introduce several indexes to investigate the effectiveness of our proposed method, which includes the contour error, the overshoot over the acceleration bound, the calculate efficiency, and the processing time.

To make a comparison, we consider the kinematic values as follows: $V_{max} = 100mm/s$, $A_{max} = 400mm/s^2$ for the nominal case. The number N of discretizations is set to be 150 in the algorithm as that in the proposed method. For the fuzzy case, the value above is set to be the risky bound, and the slipping window are $dV = 50mm/s$, $dA = 200mm/s^2$ as that in the basic case. We implement the nominal case to obtain the tracking error, which will be used as the bound for the dynamic constraint as that in [3]. Moreover, input in the nominal case will be shaped using the method in [39] by applying series of n-FIR filters for higher order trajectories. Here, we choose $n = 2$ and each of the type for the filter is as lowpass response, window with Kaiser ($\beta = 0.5$), 48KHz. The initial and terminal axis velocities and axis accelerations are all zero.

To make reasonable comparison, we have to to describe how to use the previous method to achieve the same effect as the proposed method. The center issue is how to allocate the kinematic bound V_{max} and A_{max} to generate a similar effect as the proposed method. Theoretically, we should check all the pairs $(V_{\max}, A_{\max}) \in \mathscr{V} \times \mathscr{A}$ to find the optimal bound adapted to various algorithms. But this is not practical, because this pairing is infinite. In this sense, the fuzzy algorithm can reflect its unique advantages. Back to our problem itself, here we consider the detection of nodes within the confidence interval, we divide the interval into five equal parts, and then take the corresponding pair $(V_{\max}, A_{\max}) \in \mathscr{V} \times \mathscr{A}$. Considering the effect of different combinations on the results, we set the testing values for V_{max} as 60, 75, 90; for A_{max} as 250, 300, 350. $(V_{\max}, A_{\max}) \in \{(60, 250), (75, 300), (90, 350), (60, 350), (90, 250)\}$. These pairs will be used for algorithm in [3] and [39]. To be specified, the bound of tracking error in [3] is set according to these pairs as well, which is generated after first implemented by the algorithm in [3] and record the simulation error by Simulink in Matlab. The results for these two methods are shown in Table.(II) and Table.(III).

After the previous methods, we select the "good" pair from Table.(II) and Table.(III) to make a further comparison with the fuzzy bound algorithm, which is shown in Table.(IV). Overall, from Table.(III) we can view that the FIR method can achieve a smoothing effect on acceleration without significantly increasing processing time, thereby reducing vibration. However, the FIR method greatly increases the contour error due to the introduction of a time-lag factor. Viewed from Table.(II), the dynamic constraint method can fundamentally eliminate the hidden danger of acceleration beyond the bounds. The very reason is due to the fact that the dynamic constraints is bang-bang which entail the reduction of acceleration. However, the cost is increased processing time and reduced algorithm efficiency. From the comparison results of the final three algorithms in Table.(IV), in addition to the acceleration curve vibration, the fuzzy bound (FB) method does not completely achieve zero overshoot, but it will also reduce the out-of-bounds effect to some extent as N increases. Considering the bounds obtained in practice, the curve obtained by FB method is also safe. Since the optimal combination we find here is approximate, in practice the process of finding the right combination through the other

TABLE II
ALGORITHM COMPARISON FOR DYNAMIC BOUND CASE

Dynamic bound	Planning time(s)	Cutting time(s)	Overshoot(%)	Contour error(mm)
(60,250)	33.04	5.02	–	9.8×10^{-3}
(75,300)	34.1	4.74	–	14×10^{-3}
(90,350)	30.23	4.10	–	16×10^{-3}
(60,350)	31.1	4.82	–	15.4×10^{-3}
(90,250)	34.0	4.23	–	21×10^{-3}

TABLE III
ALGORITHM COMPARISON FOR FIR SHAPING CASE

Dynamic bound	Planning time(s)	Cutting time(s)	Overshoot(%)	Contour error(mm)
(60,250)	–	4.75	2.5%	100×10^{-3}
(75,300)	–	4.04	2%	168×10^{-3}
(90,350)	–	3.60	3%	210×10^{-3}
(60,350)	–	4.57	3%	164×10^{-3}
(90,250)	–	3.93	2%	247×10^{-3}

TABLE IV
OVERALL ALGORITHM COMPARISON WITH $N = 150$. FB=FUZZY BOUND, DB=DYNAMIC BOUND

Model/Opt value	Planning time(s)	Cutting time(s)	Overshoot(%)	Tracking error(mm)
FB(72,269)	28.10	4.52	3%	11×10^{-3}
DB(75,300)	34.1	4.74	–	14×10^{-3}
FIR(60,350)	–	4.57	3%	164×10^{-3}

two methods will be more time-consuming. This is another advantage of the FB method. Generally speaking, the proposed method here is better than the previous two representative methods.

VII. CONCLUSION

We knew that the direct implementation of a "bang-bang" trajectory on a physical system with non-specialized controller can induce tool vibrations and overshoot of the nominal acceleration limits. This negative effect may bring about a series of serious consequences in the process of production. To circumvent the inherent limitation within the time-optimal framework, we propose a time-bound optimal model to recoil the kinematic bound and the safety of the CNC machine. Fuzzy set theory is used here to construct the flexible bound. This may be of great help while handling situations where the value of the bound is imprecise due to subjective human evaluation or to inconsistent evidence. Especially, we explore some properties of the new model, some of which are similar to the conventional ones however with its particularity. The proposed safety index not only shares a favorable property, but also its correctness is conveniently to be checked in the practice. The whole model can be reduced into a convex programming problem, which is trackable to implement the numerical algorithm. Finally, we make an experiment on a real CNC machine to verify the proposed model and the method.

As for industrial application, machine design is always difficult to change after installation. In particular, some old machine tool manufacturers may have gone bankrupt, so parts manufacturers cannot get technical support. Hence, our method is a feasible way to add preventive measures for processing risks. This situation is more pronounced, for instance, for many high-precision NC machining processes which require high-order kinematic constraints, such as jerk, jounce ([40], [41]), etc. The proposed method here can easily obtain the high-order kinematics boundary under the safety performance, so as to effectively avoid other problems in the machining process, such as vibration and so on. Also, the related domain such as the robotic manipulators can be applied to as well ([42], [43]). For some special handling tasks, such as storage robot path planning and large-scale repetitive planning strategies, it is necessary to carry out a safe and continuous working environment and meet certain efficiency. Therefore, it is an important application to use this kind of open-loop planning to find the speed boundary under the ideal safety performance. Our method also has limitations. The description of the membership function requires a large number of statistical results to complete, and there are fewer examples for reference in practice, so more estimates are often based on experience. How to efficiently estimate the membership function requires some advanced machine learning methods, which will be an important work for us in the future.

REFERENCES

[1] M. Ntemi, S. Paraschos, A. Karakostas, I. Gialampoukidis, S. Vrochidis, and I. Kompatsiaris, "Infrastructure monitoring and quality diagnosis in CNC machining: A review," *CIRP J. Manuf. Sci. Technol.*, vol. 38, pp. 631–649, Aug. 2022.

[2] Y. Fang, J. Hu, W. Liu, Q. Shao, J. Qi, and Y. Peng, "Smooth and time-optimal S-curve trajectory planning for automated robots and machines," *Mechanism Mach. Theory*, vol. 137, pp. 127–153, Jul. 2019.

[3] J.-X. Guo, K. Zhang, Q. Zhang, and X.-S. Gao, "Efficient time-optimal feedrate planning under dynamic constraints for a high-order CNC servo system," *Comput.-Aided Des.*, vol. 45, no. 12, pp. 1538–1546, Dec. 2013.

[4] H.-J. Zimmermann, *Fuzzy Set Theory—And Its Applications*. Cham, Switzerland: Springer, 2011.

[5] G. Li, H. Liu, W. Yue, and J. Xiao, "Feedrate scheduling of a five-axis hybrid robot for milling considering drive constraints," *Int. J. Adv. Manuf. Technol.*, vol. 112, nos. 11–12, pp. 3117–3136, Feb. 2021.

[6] F. Liang, G. Yan, and F. Fang, "Global time-optimal B-spline feedrate scheduling for a two-turret multi-axis NC machine tool based on optimization with genetic algorithm," *Robot. Comput.-Integr. Manuf.*, vol. 75, Jun. 2022, Art. no. 102308.

[7] J. Yang, D. Aslan, and Y. Altintas, "A feedrate scheduling algorithm to constrain tool tip position and tool orientation errors of five-axis CNC machining under cutting load disturbances," *CIRP J. Manuf. Sci. Technol.*, vol. 23, pp. 78–90, Nov. 2018.

[8] J. Guo, Q. Zhang, X.-S. Gao, and H. Li, "Time optimal feedrate generation with confined tracking error based on linear programming," *J. Syst. Sci. Complex.*, vol. 28, no. 1, pp. 80–95, Feb. 2015.

[9] L. Consolini, M. Locatelli, and A. Minari, "A sequential algorithm for jerk limited speed planning," *IEEE Trans. Autom. Sci. Eng.*, vol. 19, no. 4, pp. 3192–3209, Oct. 2022.

[10] K. Zhao, S. Li, Z. Kang, and Z. Liu, "Smooth trajectory generation based on contour error constraint and parameter correction B-spline," *Int. J. Adv. Manuf. Technol.*, vol. 2022, pp. 1–15, Apr. 2022.

[11] H. Li et al., "A novel feedrate scheduling method based on sigmoid function with chord error and kinematic constraints," *Int. J. Adv. Manuf. Technol.*, vol. 2022, pp. 1–22, Mar. 2022.

[12] W. Singhose, "Command shaping for flexible systems: A review of the first 50 years," *Int. J. Precis. Eng. Manuf.*, vol. 10, no. 4, pp. 153–168, Oct. 2009.

[13] W. Singhose and J. Vaughan, "Reducing vibration by digital filtering and input shaping," *IEEE Trans. Control Syst. Technol.*, vol. 19, no. 6, pp. 1410–1420, Nov. 2011.

[14] S. Tajima, B. Sencer, and E. Shamoto, "Accurate interpolation of machining tool-paths based on FIR filtering," *Precis. Eng.*, vol. 52, pp. 332–344, Apr. 2018.

[15] D. Lyu, Q. Liu, H. Liu, and W. Zhao, "Dynamic error of CNC machine tools: A state-of-the-art review," *Int. J. Adv. Manuf. Technol.*, vol. 106, nos. 5–6, pp. 1869–1891, Jan. 2020.

[16] Z. Wang, C. Hu, and Y. Zhu, "Double Taylor expansion-based real-time contouring error estimation for multiaxis motion systems," *IEEE Trans. Ind. Electron.*, vol. 66, no. 12, pp. 9490–9499, Dec. 2019.

[17] M. Chen, Y. Sun, and J. Xu, "A new analytical path-reshaping model and solution algorithm for contour error pre-compensation in multi-axis computer numerical control machining," *J. Manuf. Sci. Eng.*, vol. 142, no. 6, Jun. 2020, Art. no. 061006.

[18] Y. Chen, G. Zhang, and Y. Ran, "Risk analysis of coupling fault propagation based on meta-action for computerized numerical control (CNC) machine tool," *Complexity*, vol. 2019, pp. 1–11, Jul. 2019.

[19] S. Shuguang, Z. Wenjie, Z. Meng, L. Xiyu, and M. Xiaowan, "Fault analysis of CNC equipment based on DEMATEL/ISM/ANP," *J. Mech. Sci. Technol.*, vol. 34, no. 8, pp. 3181–3188, Aug. 2020.

[20] Y. Zhang, L. Mu, G. Shen, Y. Yu, and C. Han, "Fault diagnosis strategy of CNC machine tools based on cascading failure," *J. Intell. Manuf.*, vol. 30, no. 5, pp. 2193–2202, Jun. 2019.

[21] S. Sun, Y. Han, M. Zhang, X. Liu, G. Shen, and X. Guan, "Correlative failure analysis of CNC equipment based on SNA," *Prod. Manuf. Res.*, vol. 9, no. 1, pp. 103–115, Jan. 2021.

[22] H.-W. Lo, W. Shiue, J. J. H. Liou, and G.-H. Tzeng, "A hybrid MCDM-based FMEA model for identification of critical failure modes in manufacturing," *Soft Comput.*, vol. 24, no. 20, pp. 15733–15745, Oct. 2020.

[23] M. Kevin, "Risk assessment of computer numerical control (CNC) machine service quality," *Amer. J. Mech. Ind. Eng.*, vol. 6, no. 1, pp. 7–16, 2021.

[24] R. Ahmad and P. Plapper, "Generation of safe tool-path for 2.5D milling/drilling machine-tool using 3D ToF sensor," *CIRP J. Manuf. Sci. Technol.*, vol. 10, pp. 84–91, Aug. 2015.

[25] Y. Xiong, J. Wu, C. Deng, and Y. Wang, "Machining process parameters optimization for heavy-duty CNC machine tools in sustainable manufacturing," *Int. J. Adv. Manuf. Technol.*, vol. 87, nos. 5–8, pp. 1237–1246, Nov. 2016.

[26] L. Rattunde, I. Laptev, E. D. Klenske, and H.-C. Möhring, "Safe optimization for feedrate scheduling of power-constrained milling processes by using Gaussian processes," *Proc. CIRP*, vol. 99, pp. 127–132, Jan. 2021.

[27] F. Berkenkamp, A. Krause, and A. P. Schoellig, "Bayesian optimization with safety constraints: Safe and automatic parameter tuning in robotics," *Mach. Learn.*, vol. 112, no. 10, pp. 1–35, 2021.

[28] D. Johansson, S. Hägglund, V. Bushlya, and J.-E. Ståhl, "Assessment of commonly used tool life models in metal cutting," *Proc. Manuf.*, vol. 11, pp. 602–609, Jan. 2017.

[29] G. M. Krolczyk, P. Nieslony, and S. Legutko, "Determination of tool life and research wear during duplex stainless steel turning," *Arch. Civil Mech. Eng.*, vol. 15, no. 2, pp. 347–354, Feb. 2015.

[30] B. Mills, *Machinability of Engineering Materials*. Cham, Switzerland: Springer, 2012.

[31] G. Martínez-Arellano, G. Terrazas, and S. Ratchev, "Tool wear classification using time series imaging and deep learning," *Int. J. Adv. Manuf. Technol.*, vol. 104, nos. 9–12, pp. 3647–3662, Oct. 2019.

[32] D. J. Lin, *Multi-Objective Optimization Theory and Method*, vol. 1. Changchun, China: Jilin Education, 1992, pp. 66–67.

[33] Y. Alipouri, M. H. Sebt, A. Ardeshir, and M. H. F. Zarandi, "A mixed-integer linear programming model for solving fuzzy stochastic resource constrained project scheduling problem," *Oper. Res.*, vol. 20, no. 1, pp. 197–217, Mar. 2020.

[34] R. Ghanbari, K. Ghorbani-Moghadam, N. Mahdavi-Amiri, and B. De Baets, "Fuzzy linear programming problems: Models and solutions," *Soft Comput.*, vol. 24, no. 13, pp. 10043–10073, Jul. 2020.

[35] N. Balouka and I. Cohen, "A robust optimization approach for the multi-mode resource-constrained project scheduling problem," *Eur. J. Oper. Res.*, vol. 291, no. 2, pp. 457–470, Jun. 2021.

[36] G. Singh, M. Rattan, S. S. Gill, and N. Mittal, "Hybridization of water wave optimization and sequential quadratic programming for cognitive radio system," *Soft Comput.*, vol. 23, no. 17, pp. 7991–8011, Sep. 2019.

[37] M. V. Bobyr, A. S. Yakushev, and A. A. Dorodnykh, "Fuzzy devices for cooling the cutting tool of the CNC machine implemented on FPGA," *Measurement*, vol. 152, Feb. 2020, Art. no. 107378.

[38] M. V. Bobyr, N. A. Milostnaya, and V. A. Bulatnikov, "The fuzzy filter based on the method of areas' ratio," *Appl. Soft Comput.*, vol. 117, Mar. 2022, Art. no. 108449.

[39] B. Sencer, K. Ishizaki, and E. Shamoto, "High speed cornering strategy with confined contour error and vibration suppression for CNC machine tools," *CIRP Ann.*, vol. 64, no. 1, pp. 369–372, 2015.

[40] A. Bharathi and J. Dong, "Feedrate optimization for smooth minimum-time trajectory generation with higher order constraints," *Int. J. Adv. Manuf. Technol.*, vol. 82, nos. 5–8, pp. 1029–1040, Feb. 2016.

[41] L. Zhang and J. Du, "Acceleration smoothing algorithm based on jounce limited for corner motion in high-speed machining," *Int. J. Adv. Manuf. Technol.*, vol. 95, nos. 1–4, pp. 1487–1504, Mar. 2018.

[42] A. Palleschi, M. Garabini, D. Caporale, and L. Pallottino, "Time-optimal path tracking for jerk controlled robots," *IEEE Robot. Autom. Lett.*, vol. 4, no. 4, pp. 3932–3939, Oct. 2019.

[43] Z. Chen, J. Liu, and F. Gao, "Real-time gait planning method for six-legged robots to optimize the performances of terrain adaptability and walking speed," *Mechanism Mach. Theory*, vol. 168, Feb. 2022, Art. no. 104545.